Flux creep in iron-doped Y-Ba-Cu-O single crystals

M. D. Lan, J. Z. Liu, and R. N. Shelton
Department of Physics, University of California at Davis, Davis, California 95616-8677
(Received 13 August 1990; revised manuscript received 2 April 1991)

We report the zero-field-cooled magnetic relaxation and thermal activation energy in various $YBa_2Cu_{3-x}Fe_xO_7$ single crystals. No subgranularity effects were observed in our single crystals. The phenomenon of giant flux creep is evident in these systems. The magnetic relaxation rate $dM/d(\ln t)$ is strongly dependent on temperature and applied magnetic field. We utilize the Anderson-Kim thermally activated flux-creep model to analyze these systems.

INTRODUCTION

Since the discovery of high-T_c superconductors,[1-3] scientists have spent significant effort to improve the critical current density J_c. Unfortunately, there is a substantial problem of "flux-lattice melting" in many of the high-T_c superconductors.[4] The severe motion of the flux lines causes the decay of supercurrent with time, which limits the usefulness of high-T_c superconductors. Based on numerous studies, it is generally agreed that strong defect pinning centers for the flux lines are required for the enchancement of J_c. Hence, during the last few years the pinning and flow of flux lines in the mixed state of such superconductors have been studied intensively.[5-7]

According to dc magnetization measurements in $YBa_2Cu_{3-x}Fe_xO_7$ single crystals, the Meissner fraction decreases as a small amount of Cu is substituted by Fe.[8] This effect suggests the pinning in iron-doped systems could be improved. Therefore, either from the fundamental research or practical application of point of view, it is desirable to know the strength of flux pinning and the thermal activation energy U_0 in various iron-doped $YBa_2Cu_3O_{7-y}$ (Y-Ba-Cu-O) materials. In addition, it is also important to apply a theoretical model, which can give a consistent explanation of the data to experimental results. From that point of view, we provide relevant experimental information to fit theoretical models and provide a further understanding of the underlying mechanism of high-T_c superconductors.

Two elegant theoretical models are generally used to interpret this type of experimental result in both low-T_c and high-T_c superconductors. One is the flux-creep model developed by Anderson and Kim.[9,10] The Anderson-Kim thermal activated flux-creep model has been successfully applied to explain the dynamic flow of flux lines in conventional type-II superconductors.[11] Due to the extremely short coherence length (ξ) and high transition temperature as compared with conventional type-II superconductors, it is anticipated that Y-Ba-Cu-O and its derivative systems will have giant flux-creep effects.[5,12] Another model is derived from the observation of an irreversible line in oxide superconductors. The behavior of magnetic irreversibility, $(T-T_c)\propto H^{2/3}$, is analogous to that of spin-glass systems. The Ebner-Stroud superconducting glass model,[13] which starts from a picture of a random distribution of Josephson weak-links, was already used to explain many of the experimental phenomena in Y-Ba-Cu-O-type superconductors. It is interesting to test and compare the applicability of these two theoretical models to high-T_c superconducting single crystals.

The possible existence of Josephson weak links in $YBa_2Cu_{3-x}Fe_xO_7$ materisls, even single crystals, is still controversial. As a result, it is very important to determine which picture, either the Ebner-Stroud superconducting glass model or the Anderson-Kim flux-creep model, is more suitable. From the published result of transmission electron microscopy (TEM), it is known that in $YBa_2Cu_{3-x}Fe_xO_7$ the separation of twin boundaries is less than 20 nm for $x=0.06$ while it is about 200 mn in the pure $YBa_2Cu_3O_7$ system.[14,15] The twin boundaries disappear for $x>0.1$. The presence of twin boundaries which occurs in the orthorhombic phase of $YBa_2Cu_{3-x}Fe_xO_7$ is one of the possible origins of the subgranular structure in single crystals. Therefore, the noticeable difference in twin boundary density between the pure and iron-doped Y-Ba-Cu-O specimens provides a useful means for testing these two theoretical models.

Here we report systematic measurements of the magnetic relaxation over wide temperature and magnetic field ranges for various iron-doped Y-Ba-Cu-O single crystals. In most applied fields and temperatures, the magnetization decays logarithmically in time. It is similar to either the flux-creep phenomenon observed in conventional hard superconductors, or the glassy behavior resulting from the presence of weak links. In this paper we also focus on the comparison of the zero-field-cooled magnetic relaxation and the thermal activation energy between pure $YBa_2Cu_3O_7$ and low iron composition $YBa_2Cu_{3-x}Fe_xO_7$ systems.

EXPERIMENTAL DETAILS

Due to the large anisotropy in oxide superconductors and the presence of weak links between grain boundaries, polycrystalline samples are not suitable materials for these studies. All of our experiments were done on selected regular-shaped $YBa_2Cu_{3-x}Fe_xO_7$ single crystals.

Single crystals were grown by using a modified self-flux technique with excess CuO as flux.[16,17] These specimens are rectangular slabs with iron composition, dimensions and midpoint of the inductive transition temperature listed in the Table I. The iron composition x varies from zero to 0.24. In Table I, the reduced dimension d is defined as $b(1-b/3a)$, where a and b are the sample dimensions in the CuO plane and $a>b$ in our definition. The applied magnetic field is along the c axis, so that the flux lines can be parallel to the twin boundaries. The extremely sharp inductive transition and 100% diamagnetism[8] indicate the high quality of these single crystals. Based on the polycrystalline work in $YBa_2Cu_{3-x}Fe_xO_7$ systems, the variation in oxygen content due to the presence of iron is insignificant with respect to superconductivity and electronic properties since the iron composition is so small ($x<0.24$). Therefore, we assume the oxygen contents in our single crystals are constant.

To investigate the subgranularity effect, we cut original pieces of single crystals labeled no. 2 and no. 5 in Table I into smaller sizes (sample no. 3, no. 4 from no. 2 and sample no. 6 from no. 5) and remeasured the hysteresis loop. The whole hysteresis loop is obtained by measuring the magnetization 1 min after the field reaches stability as the magnetic field is varied from zero to 5.5 T, swept to -5.5 T, then back to 5.5 T. Measurements at each field are made with magnet in the persistence mode. According to the Bean critical model, in the case of the magnetic field applied along the c axis, the critical current density J_c can be derived from

$$J_c=\frac{20\Delta M}{d},$$

where d is the reduced dimension and ΔM is the magnetization difference between the increasing field and decreasing field. A subgranularity effect is observed if the width of hysteresis loop remains the same as the sample's reduced dimension d changes.

In order to test the thermally activated flux-creep model, measurements of evanescent decay of the magnetization are carried out in the temperature range of 5 K to T_c and for magnetic fields up to 5 T. A standard superconducting quantum interference device (SQUID) magnetometer[18] is used to measure the magnetization. Most of the temperature dependence relaxation rates are obtained at the applied magnetic fields of 500 Oe and 1 T. With the demagnetization factor D of about 0.9 for the magnetic field along the c axis, our applied field is well above the lower critical field, H_{c1}, at all temperatures. Field dependence relaxation rates are obtained at $T=6$ K with fields applied perpendicular to the CuO plane. All data are taken by applying the magnetic field after the sample is cooled down to the superconducting state (ZFC) and the temperature is stabilized.

EXPERIMENTAL RESULTS AND DISCUSSIONS

From Fig. 1 and Table I, it is clear that the magnetization difference ΔM between increasing field and decreasing field is linearly proportional to the reduced dimension. The slope of each curve indicates the size of critical current density within a proportionality constant. These data indicate that the critical current density at $T=5$ K and $H=1$ T decreases as the iron composition increases and no subgranular weak links exist in our $YBa_2Cu_{3-x}Fe_xO_7$ single crystals.

In Fig. 2 we illustrate the typical change of magnetization with time in different magnetic fields for the $YBa_2Cu_{2.94}Fe_{0.06}O_7$ single crystal. A strong logarithmic decay of the zero-field-cooled magnetization was observed in the relaxation measurement. In the low field regime, the magnetization displays an erratic decay with a large fluctuation which might be related to instable flux jumps and surface effects. The time dependence of the magnetization in different applied fields shows a logarithmic decay with various slopes. The slope $dM/d(\ln t)$ is then defined as the magnetic relaxation rate, which also represents the decay rate of the supercurrent. The field dependence of the relaxation rate is plotted in Fig. 3. In the low applied field range, $(1-D)H_{c1}<H_a<H_a^*\equiv(1-D)H^*$, the flux does not penetrate through the whole sample and the relaxation rate increases quadratically with the increasing field. Here H^* is the local field at which the flux fronts overlap in the sample. Experimentally, H_a^* is the applied field at which the maximum diamagnetism occurs in the hysteresis loop measurement. The value of H_a^* is strongly dependent on the geometrical shape of the sample and is estimated on the order of $0.2\pi(1-D)dJ_c$.[7] We denote the experimental values of H_a^* by arrows in Fig. 3. When the applied field is greater than H_a^*, current flows through the entire volume of the single crystal and the magnetic relaxation rate decreases slightly. The crossover between these two regions is broad and that could be due to the asymmetry of the

TABLE I. Dimensions and composition of $YBa_2Cu_{3-x}Fe_xO_7$ single crystals used in magnetic measurements. The data of magnetization difference is taken at $T=5$ K and $H=1$ T.

Sample no.	x	T_c(K)	Dimension(mm^3)	d(mm)	ΔM(emu/cm^3)
1	0	91.2	0.7×0.6×0.045	0.428	4512
2	0.06	82.1	1.2×1.0×0.040	0.722	6048
3	0.06	82.1	0.8×0.7×0.040	0.496	3979
4	0.06	82.1	0.8×0.3×0.040	0.263	2173
5	0.12	76.0	1.0×0.8×0.023	0.587	2459
6	0.12	76.0	0.6×0.5×0.023	0.361	1468
7	0.24	48.3	0.9×0.8×0.022	0.936	716

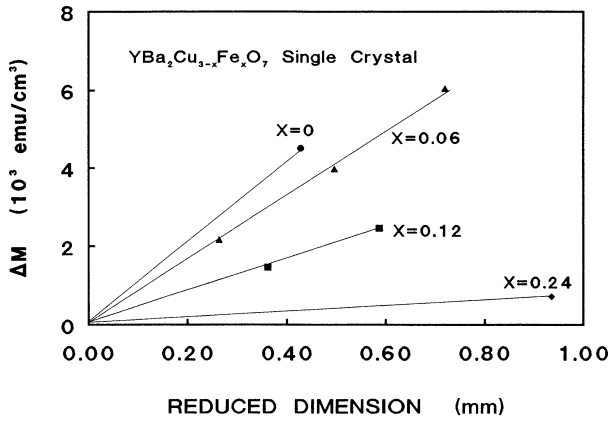

FIG. 1. Magnetization difference between increasing field and decreasing field as a linear function of reduced dimension of $YBa_2Cu_{3-x}Fe_xO_7$ single crystals at $T=5$ K and $H=1$ T. The applied field is along the c axis. The slope for each curve is proportional to the critical current density.

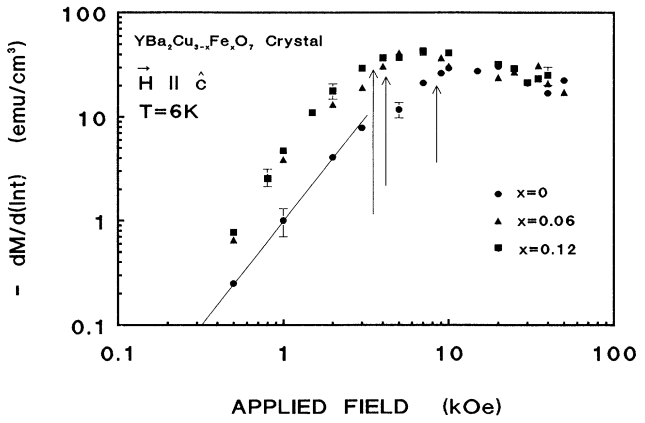

FIG. 3. Field dependence of the magnetic relaxation rate in $YBa_2Cu_{3-x}Fe_xO_7$ single crystal for $T=6$ K. H_a^* indicated by arrows are from hysteresis loop measurements for various compositions. The solid line is the best quadratic fitting for $H_a < H_a^*$.

crystal. More detailed information of the flux configuration inside the specimen is required to understand the broadness of the peak. The data shown in Fig. 3 can be interpreted by the classic Anderson-Kim thermal activated flux-creep model. For $(1-D)H_{c1} < H_a < H_a^*$ and $kT \ll U_0$, the magnetic relaxation developed by Beasley *et al.*[11] can be expressed as

$$\frac{dM}{d(\ln t)} = \left[\frac{kT}{U_0}\right]\left[\frac{1}{64\pi^2 M_0}\right]H_a^2$$

and

$$\frac{dM}{d(\ln t)} = \left[\frac{kT}{U_0}\right]M_0$$

for $H_a > H_a^*$, where U_0 is the thermal activation energy in the absence of a flux gradient, and M_0 is the irreversible magnetization in the absence of the thermal activated motion. We can also express M_0 by $dJ_{c0}/40$ where J_{c0} is the critical current density without the thermal activated motion. For consistency we select M_0 as the value extrapolated to $t=1s$ after field application. In Fig. 3 the lower critical field can also be obtained from the onset of flux penetration when the applied field H_a is above the threshold $H_{c1}(1-D)$. The value of H_{c1} at 6 K and H∥c axis obtained from this method is about 2.3 kOe for $x=0$, 1.68 kOe for $x=0.06$ and 1.5 kOe for $x=0.12$. These results are consistent with the estimated values from the method of the deviation from perfect diamagnetism in the magnetization versus field curve.

The temperature dependence of the zero-field-cooled $dM/d(\ln t)$ in the low field region is shown in Fig. 4. Our data show a peak around 15 K to 35 K for various iron

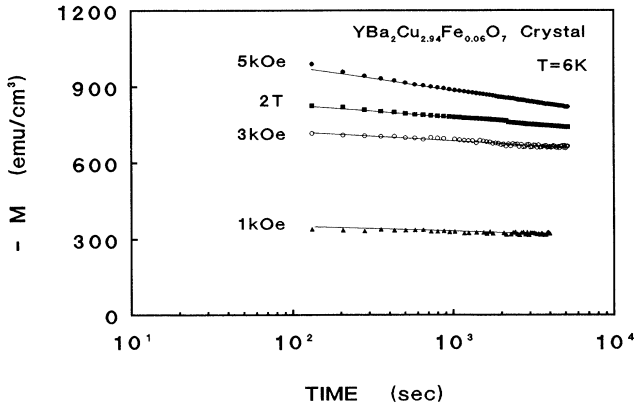

FIG. 2. Typical decay of magnetization with time under different magnetic fields in $YBa_2Cu_{2.94}Fe_{0.06}O_7$ single crystal (sample no. 4).

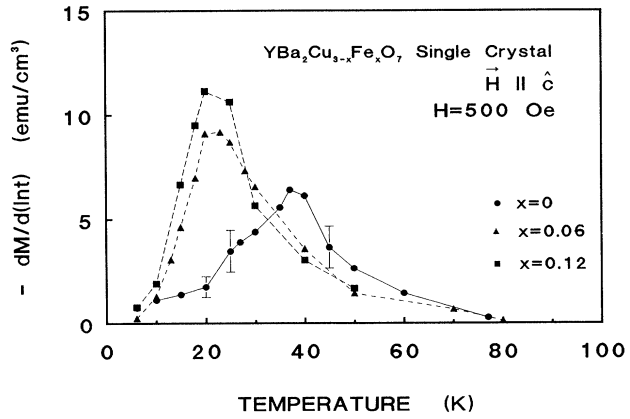

FIG. 4. Temperature dependence of the magnetic relaxation rate in $YBa_2Cu_{3-x}Fe_xO_7$ single crystal. The applied field is 0.5 kOe. Lines which connect data points are only a guide to the eye.

compositions. The peak position tends to shift to lower temperature as the iron composition increases. As explained in the work of Yeshurun and Malozemoff,[5] the maximum relaxation rate is due mainly to the competition of the monotonically increasing temperature dependence and the decrease of the ratio of J_{c0}/U_0 with increasing temperature. If we simply assume $J_{c0}/U_0 \propto (T_c - T)^m$, then the peak in the relaxation rate versus temperature graph occurs at $[1/(m+1)]T_c$. Based on that argument, m is about 1.5 for pure Y-Ba-Cu-O and about 4 for iron-doped samples at $H_a = 0.5$ kOe. This result suggests a stronger temperature dependence of the critical current density in iron doped samples. However, this conclusion may be too simplistic if the actual temperature dependence in J_{c0} and U_0 is more complicated than assumed in this model. In the low temperature regime, 0.5 kOe is too low to have the current density equal to the critical density in the whole specimen. In order to have a full critical state over the entire temperature range, we carry out the same relaxation measurements in an applied field of 1 T. The typical magnetization versus time data for various temperatures are displayed in Fig. 5. We observe a remarkable logarithmic decay in the magnetizations. The decay rate $dM/d(\ln t)$ gradually changes from about 22 emu/cm^3 at 5 K to few emu/cm^3 at high temperature for the $x = 0.12$ sample. The decay rate corresponds to about 3 to 5% reduction per order of magnitude change in time. It is a significant phenomenon in comparison with traditional type-II superconductors. The decay rates for the pure and other iron-doped samples also show a similar behavior. In comparison among these samples with different iron compositions, we found that the decay rate is relatively smaller in the iron-doped samples (Fig. 6). The decay rate reaches a maximum of about 10 K for pure Y-Ba-Cu-O, but a maximum is not observed down to 5 K in doped samples. The shift of the peak position toward lower temperature could be due to the stronger temperature dependence of J_{c0}/U_0 at high field. That is also the possible reason why a peak is not observed in iron doped

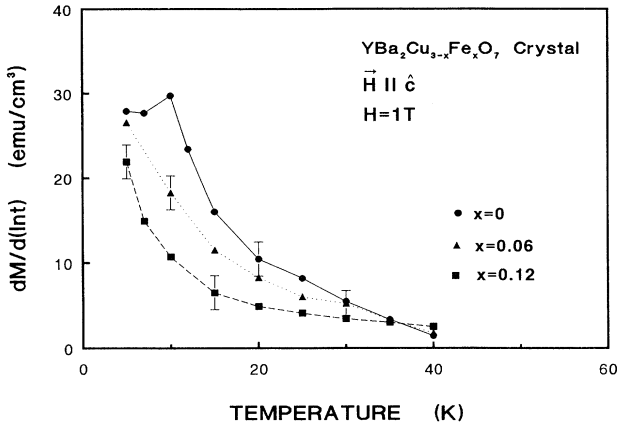

FIG. 6. Temperature dependence of magnetic relaxation rate in $YBa_2Cu_{3-x}Fe_xO_7$ single crystal. The applied field is 1 T. Lines connecting data points are only a guide to the eye.

samples. Another interesting observation is the finite value of $dM/d(\ln t)$, even normalized by the initial magnetization M_0, when extrapolating to zero temperature. This phenomenon is not easy to understand whether the framework of a classic thermally activated flux motion model. Griessen *et al.* suggest quantum flux line tunneling among pinning regions (see Ref. 22) in their thin film experiment. Due to the short superconducting coherence length in our $YBa_2Cu_{3-x}Fe_xO_7$ systems, this seems to be an acceptable explanation.

Based on the relaxation equation in the full critical state ($H_a > H_a^*$), we obtain the thermal activation energy U_0 from the slope and the intercept in the semilogarithmic plot of diamagnetic moment versus time. The general feature of these data, summarized in Fig. 7, indicates that U_0 tends to increase rapidly with temperature. In addition, the effective activation barrier is increasing as the iron composition increases. The difference of U_0 between

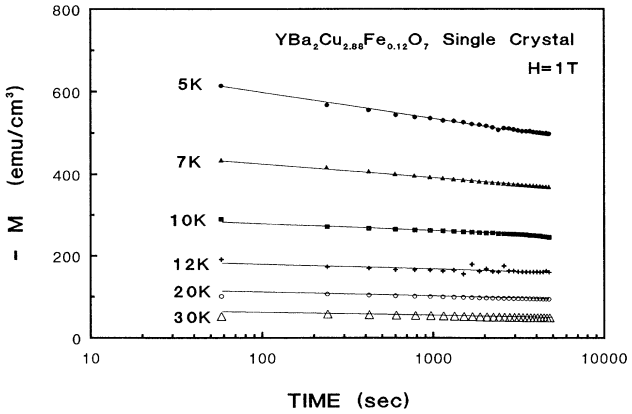

FIG. 5. Typical decay of magnetization with time under different temperatures in $YBa_2Cu_{2.88}Fe_{0.12}O_7$ single crystal. The applied field is 1 T.

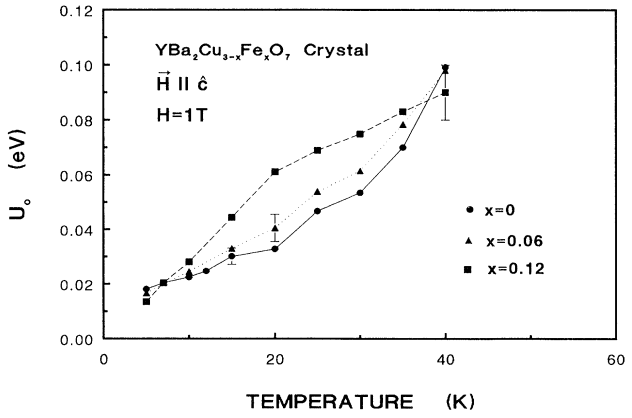

FIG. 7. Temperature dependence of the thermal activation energy in $YBa_2Cu_{3-x}Fe_xO_7$ single crystals. The applied field is 1 T.

the pure and low composition iron-doped specimens might be caused by the increasing twin boundary and the boundary width. However, the critical current density J_c for different iron compositions shows the opposite trend in comparison to the thermal activation energy. The resolution of this problem is connected to the anisotropy in J_c and U_0 in Y-Ba-Cu-O crystals. It is well known that the pinning barrier in Y-Ba-Cu-O single crystal is larger for $\mathbf{H}\|\mathbf{c}$ axis than for $\mathbf{H}\|ab$ plane; however, the anisotropic J_c reported by many research groups is opposite.[19] Actually, J_c is related more independently to the pinning force F_p than to the pinning potential.[1] Therefore, the opposite trend in J_c and U_0 must come from the difference in the characteristic length for the pinning barrier l and the activation volume V_a. The activation volume is proportional to ξ^3 in low field and $a_0^2\xi$ in high fields. Here ξ is the Ginzburg-Landau coherence length and a_0 is the separation between flux lines. For an applied field of 1 T, the distance between flux lines a_0 is about 50 nm, which is smaller than the penetration depth λ for all iron-doped samples. Thus these experimental conditions are in the high field limit. Furthermore, if we take twin boundary efforts into account and assume the twin boundaries are effective pinning centers, then l should be selected as the separation of the twin boundaries. The separation of twin boundaries is ten times smaller in low composition iron-doped samples than pure Y-Ba-Cu-O. Therefore, even though the coherence length for iron-doped material is a factor of 2 larger than in pure Y-Ba-Cu-O, the dramatic reduction in the average hopping distance (l) determined by twin boundary spacing, should result in an enhancement of J_c. Since this does not occur we conclude that the twin boundaries are not effective pinning centers in the $YBa_2Cu_{3-x}Fe_xO_7$ system. This uneffectiveness is due to the mismatch of the coherence length and twin width (defect size). For the field perpendicular to the ab plane, the thermal activation energy U_0, obtained in the $YBa_2Cu_{3-x}Fe_xO_7$ system is about 20 meV at 5 K and goes up to 100 meV at 40 K. These values are comparable to the result from other research groups, such as Yeshurun[20] and Stollman.[21]

Hagen and Griessen *et al.* discussed the relaxation of the magnetization using Monte Carlo simulation.[22,23] In their model the magnetization has a linear decay at very short times and an exponential decay at very long times with the crossover occurring at a characteristic time t^*. For most experimental time scales ($10-10^4$ s), a logarithmic decay of the magnetization is predicted. In our experiments, the magnetization relaxation basically follows a logarithmic dependence except in the very beginning ($t > 100$ s). Within that time region, the nonlogarithmic magnetic relaxation process could be due to surface effects. In addition, the characteristic time t^* used to separate the logarithmic and exponential decay regimes for our experimental temperature range are far away from our experimental time scale, so the exponential regime cannot be reached. Although the exponential decay regime is expected to be easily attainable for the temperature near T_c, the magnetization signal in the high temperature regime is very small. Thus, it is difficult to test the validity of their model from our current data.

CONCLUSION

We have reported the field and temperature dependence of zero-field-cooled magnetic relaxation rates in various Fe-substituted $YBa_2Cu_3O_7$ single crystals. This study improves our understanding of the classical flux-creep process in new oxide superconducting systems. The behavior of the magnetic flux shows good agreement with the theoretical predictions of the Anderson-Kim model.[9,10] We also compare the relaxation rate and the strength of the pinning sites in various single crystals with different twin boundary densities. The results do not show an unusually strong activation potential in high twin-boundary density systems. This is consistent with the observation of decreasing critical current density in iron-doped systems at 1 T. The twin boundaries in $YBa_2Cu_{3-x}Fe_xO_7$ single crystals do not act as effective pinning centers for flux lines.

No subgranular effects were observed in our magnetic measurement on $YBa_2Cu_{3-x}Fe_xO_7$ single crystals. This suggests that the superconducting-glass model is not relevant to our single crystals; however, it could still be an appropriate model for the ceramic materials where the grain boundary acts as a weak link. The Anderson-Kim flux-creep picture is a suitable model in explaining our single-crystal data. A single thermal activation energy derived from Beasley's formula cannot satisfactorily explain the behavior in terms of the flux pinning model. Rather, a distribution of activation energies is more realistic to interpret the observed temperature dependence of U_0.

ACKNOWLEDGMENTS

This research was performed under the auspices of the U.S. Department of Energy for Lawrence Livermore National Laboratory under grant Contract No. W-7405-ENG-48.

[1] J. G. Bednorz and K. A. Müller, Z. Phys. B **64**, 189 (1986).

[2] M. K. Wu, J. R. Ashburn, C. J. Torng, P. H. Hor, R. L. Meng, L. Gao, Z. J. Huang, Y. Q. Wang, and C. W. Chu, Phys. Rev. Lett. **58**, 908 (1987).

[3] C. W. Chu. Ph. H. Hor, R. L. Meng, L. Gao, K. J. Huang, and Y. Q. Wang, Phys. Rev. Lett. **58**, 405 (1987).

[4] J. D. Hettinger, A. G. Swanson, W. J. Skocpol, J. S. Brooks, J. M. Graybeal, P. M. Mankiewich, R. E. Howard, B. L. Stranghn, and E. G. Burkhardt, Phys. Rev. Lett. **62**, 2044 (1989).

[5] Y. Yeshurun and A. P. Malozemoff, Phys. Rev. Lett. **60**, 2202 (1988).

[6]M. Tinkman, Phys. Rev. Lett. **61**, 1658 (1988).
[7]A. P. Malozemoff, T. K. Worthington, R. M. Yandrofski, and Y. Yeshurun, in *Towards the Theoretical Understanding of High Temperature Superconductors,* edited by S. Lundquist (World Scientific, Singapore, 1988).
[8]M. D. Lan, J. Z. Liu, and R. N. Shelton (unpublished).
[9]P. W. Anderson, Phys. Rev. Lett. **9**, 309 (1962).
[10]P. W. Anderson and Y. B. Kim, Rev. Mod. Phys. **36**, 39 (1964).
[11]M. R. Beasley, R. Labusch, and W. W. Webb, Phys. Rev. **181**, 682 (1969).
[12]A. M. Campbell and J. E. Evetts, Adv. Phys. **21**, 199 (1972).
[13]C. Ebner and D. Stroud, Phys. Rev. B **31**, 165 (1987).
[14]Youwen Xu, M. Suenaga, J. Tafto, R. L. Sabatini, A. R. Moodenbaugh, and P. Zolliker, Phys. Rev. B **39**, 6667 (1989).
[15]Y. Zhu, M. Suenaga, Youwen Xu, R. L. Sabatini, and A. R. Moodenbaugh, Appl. Phys. Lett. **54**, 374 (1989).
[16]J. Z. Liu, G. W. Crabtree, A. Umezawa, and Li Zongquan, Phys. Lett. **121**, 305 (1987).
[17]D. L. Kaiser, F. Holtzberg, B. A. Scott, and T. R. Mcguire, Appl. Phys. Lett. **51**, 1040 (1987).
[18]Quantum Design, Inc., San Diego, CA.
[19]G. W. Crabreee, J. Z. Liu, A. Umezawa, W. K. Kwok, C. H. Sowers, S. K. Malik, B. W. Veal, D. J. Lam, M. B. Brodsky, and J. W. Downey, Phys. Rev. B **36**, 4021 (1987).
[20]Y. Yeshurun, A. P. Malozemoff, T. K. Worthington, R. M. Yandrofski, L. Krusin-Elbaum, F. Holtzberg, T. R. Dinger, and G. V. Chandrashekar, Cryogenics **29**, 258 (1989).
[21]G. M. Stollman, B. Dam, J. H. P. M. Emmen, and J. Pankert, Physica C **159**, 854 (1989).
[22]C. W. Hagen, R. Griessen, and E. Salomons, Physica C **157**, 199 (1989).
[23]Griessen, J. G. Lensink, T. A. M. Schröder, and B. Dam, Cryogenics **30**, 563 (1990).